Appl. Phys. B
DOI 10.1007/s00340-014-5837-7

Applied Physics B
Lasers and Optics

Two-photon fabrication of organic solid-state distributed feedback lasers in rhodamine 6G doped SU-8

W. Horn · S. Kroesen · C. Denz

Received: 9 August 2013 / Accepted: 10 April 2014
© Springer-Verlag Berlin Heidelberg 2014

Abstract We report the fabrication of distributed feedback lasers in Rhodamin 6G doped SU-8 by direct femtosecond laser writing. The devices are fabricated by point-by-point exposure and consist of a core layer with a low-order Bragg grating on the surface. A quarter-wavelength phase shift is introduced in the middle of the grating section to obtain single-mode emission. Lasing at different wavelengths is demonstrated by changing the grating pitch. Spectral emission, threshold and lifetime characterization is performed by pumping the laser with a pulsed, frequency double Nd:YAG laser.

1 Introduction

Organic solid-state lasers have gained interest in the last decades due to their broad gain spectrum, large stimulated emission cross sections, and potentially compact and low-cost fabrication with applications in miniature spectroscopy and optical sensing [1, 2]. In particular, distributed feedback (DFB) lasers [3] realized in photopolymers doped with conventional dyes have been investigated either by fabricating a permanent DFB structure [4, 5] or generating a photo-induced gain modulation during illumination with the pump pulses [6, 7]. Aside from microfluidic organic lasers, organic solid-state DFB lasers where the dye is incorporated in a polymer host material are simple and robust light sources, which can be fabricated on flexible substrates making them suitable for integration into lab-on-a-chip systems where coherent illumination is desirable. Although direct electric pumping has not been feasible so far, organic lasers can be pumped with inexpensive pulsed LEDs [8]. Due to these benefits, microcavity lasers in polymers using dye gain materials have been realized through a variety of fabrication methods such as selective etching [9], holography [10], nano-imprinting [11], UV-lithography [12] and electron/proton beam writing [13, 14]. However, fabrication of organic DFB lasers by two-photon absorption (TPA) of femtosecond radiation offers many benefits for rapid prototyping of microcavity organic lasers. One of the most attractive aspects of femtosecond fabrication is the feasibility to produce almost arbitrary three-dimensional structures with sub-micrometer features by translating the host material under the laser focal point [15]. This enables sophisticated fabrication of nonuniform gratings and three-dimensional lasing structures such as microdisk resonators with high Q-factors [16].

Until now, fabrication of DFB lasers using TPA has been reported using dendrimers [17] and inorganic-organic polymers (Ormocer) [18] as host materials with DCM as the laser dye. In this paper, we demonstrate fabrication of DFB lasers in Rhodamin 6G doped SU-8 by femtosecond laser writing. Although SU-8 exhibits a higher absorption and has a higher refractive index ($n = 1.6$ at $\lambda = 633$ nm) compared to hybrid polymers, it offers high aspect ratios, mechanical rigidity, thermal and chemical resistance and a higher two-photon cross section. Additionally, it permits arbitrary irradiation strategies since the polymerization takes place after the post-exposure bake. It has been shown for dye-doped photonic crystal lasers fabricated by nano-imprinting, that SU-8 offers some advantages over the hybrid polymer Ormocore in context of wavelength reproducibility, since Ormocore is a fluid at room temperature yielding higher surface variations [19].

W. Horn (✉) · S. Kroesen · C. Denz
Institute for Applied Physics, Center for Nonlinear Science, Münster, Germany
e-mail: w.horn@wwu.de

Published online: 20 May 2014

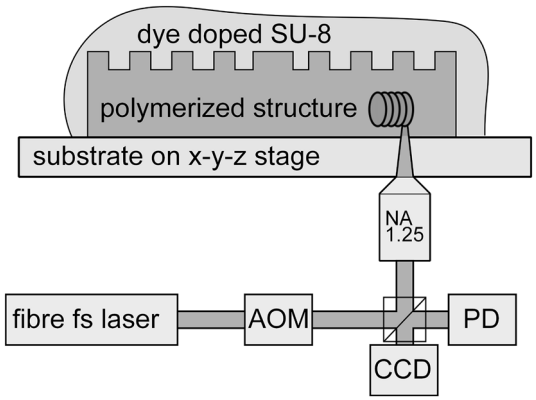

Fig. 1 Schematic setup for fabrication of a DFB laser in Rhodamin doped SU-8. The spin-coated polymer is structured by a femtosecond fiber laser, developed and subsequently pumped with a ns-pulselaser. The spectral emission is read out with a fiber-coupled grating spectrometer. *AOM* acousto optic modulator, *PD* photodiode, *CCD* camera

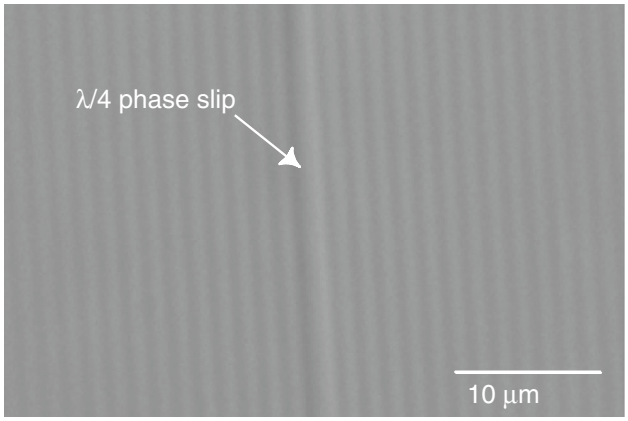

Fig. 2 Top-view phasecontrast image of a fabricated DFB laser taken with an optical microscope at ×100 magnification where the phase slip is clearly visible in the middle

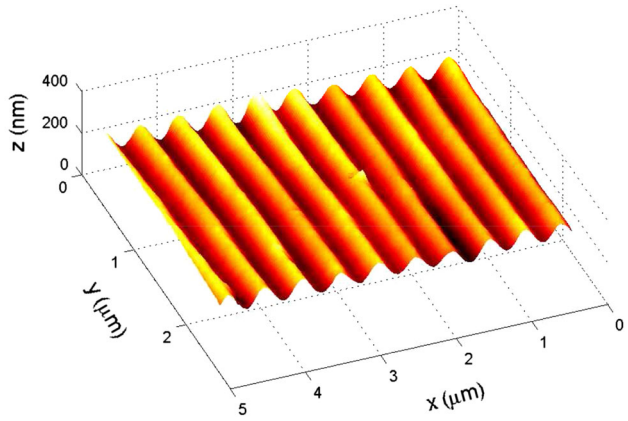

Fig. 3 Atomic force microscope height profile of the corrugated surface with a total length of 100 µm. The periodicity is 550 nm and the surface modulation is 80 ± 5 nm

2 Device fabrication

For fabrication of the devices, the Rhodamin 6G dye was dissolved in ethanol (approx. 5 mg/ml) by mixing SU-8-100 (MicroChem) was mixed with Rhodamin 6G and put into an ultrasonic bath for 60 min to obtain a homogeneous solution of approximately 10 µmol/g. The solution was spin coated onto a cover slip and pre-baked for 30 min at 95 °C to evaporate the solvent. After exposure, the sample was post-baked for 10 min at 95 °C and developed with mr-Dev 600. The experimental setup for exposure and characterization of the devices is shown in Fig. 1. Exposure was carried out with a frequency-doubled femtosecond fiber laser (Toptica FemtoFiber Pro NIR) at a wavelength of 780 nm and 100 fs pulse duration at 80 MHz repetition rate. This enables TPA with high spatial resolution in the absorption band of SU-8 with a voxel size below the cubic wavelength. The samples were put on an *x*–*y*–*z* translation stage (PI Mars), and the beam was focussed by a microscope objective (NA 1.25) at the polymer/silica boundary. For the particular numerical aperture, the pulse energy and translation velocity were adjusted to achieve a third-order feedback grating period around $\Lambda = 550$ nm. The translation velocity was 50 µm/s at 10 mW power. In a first step, a core layer was rasterized into the sample with a line spacing of 100 nm yielding a large overlap of the exposed lines to obtain a seamless rectangle with a size of $20 \times 100\,\mu m^2$. The laser focus slightly overlaps with the substrate and truncates the voxels to stick the structure to the substrate. This produced an estimated core layer thickness around 700–800 nm. In a second step, a grating layer was written on top of the core layer, with a third-order grating structure through line-by-line exposure. The grating period for the desired emission wavelength λ has to satisfy the Bragg condition $\Lambda = m\lambda/(2n_{\text{eff}})$ where m is the order number, Λ is the grating pitch and n_{eff} is the effective refractive index experienced by a mode. The refractive index of undoped SU-8 is around $n = 1.6$ at 633 nm but depends on the Rhodamin concentration. Additionally, the mode field extends the cavity, thus depending on the device dimensions and reducing n_{eff}. Experimental values for n_{eff} where later derived from the measured emission spectra. Rhodamin 6G supports laser operation in a wide spectral range of more than $\Delta\lambda = 50$ nm with a maximum gain around $\lambda = 570$ nm, therefore supporting a large number of longitudinal cavity modes. To select a single mode, a feedback grating with a quarter-wave phase shifted in the middle of the grating section is introduced. Without a phase shift, the refractive index modulation leads to a mode degeneracy and results in lasing modes next to the Bragg

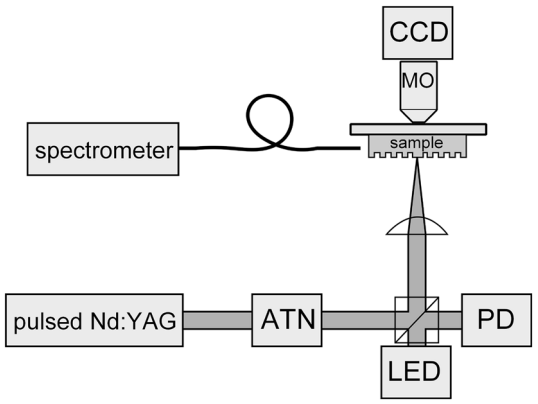

Fig. 4 Schematic setup for characterization of a dye laser. The laser is optically pumped with a ns-pulselaser, and the spectral emission is read out with a fiber-coupled grating spectrometer. The pulse energy is controlled by a photodiode, and the alignment is performed with a LED and a CCD-camer. *ATN* attenuation, *PD* photodiode, *CCD* camera, *LED* light-emitting diode, *MO* microscope objective

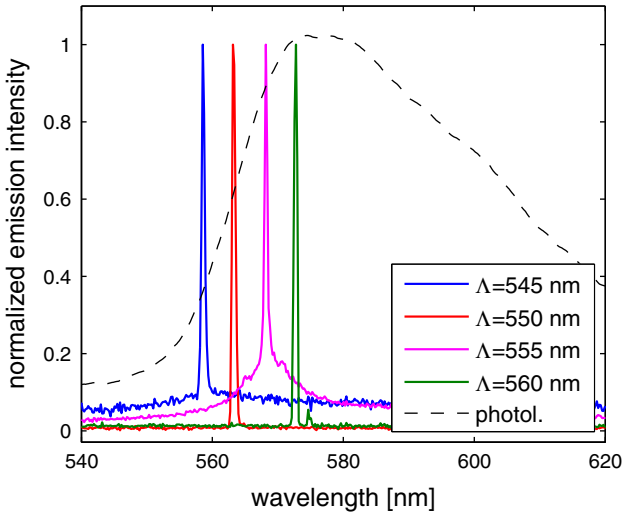

Fig. 5 Normalized emission spectra of a DFB laser array with four different grating pitches increased in 5-nm steps. The DFB devices exhibit single-mode emission. The *dashed curve* is the photoluminescent signal

frequency [20]. This holds for index coupled devices where the real part of the effective refractive index dominates the feedback mechanism [21]. However, in some cases, one of the modes may experience higher losses which still yields single-mode operation depending on the pump energy used. For a grating phase shift of $\varphi = \lambda/4$, the passband is located in the middle of the reflection spectrum [22]. The spectral response was calculated using the transfer matrix approach based on the coupled mode theory [23]. The width of the passband depends on the refractive index contrast and loss yielding values below 100 pm that could not be resolved by the fixed grating spectrometer.

Figure 2 shows a magnified view central area taken by an optical microscope where the phase slip is clearly visible. Figure 3 shows a height profile taken by an atomic force microscope of a third-order grating. The period is $\Lambda = 550\,\text{nm}$ with a modulation depth of $d = 80 \pm 5\,\text{nm}$.

3 Device characterization

Emission properties were characterized by pumping the devices with a frequency-doubled Nd:YAG laser (Coherent Infinity) at 532 nm with a pulse duration of approximately 6 ns and a stripe profile generated by a cylindric lens. The dimension of the pump spot was approximately $2 \times 0.5\,\text{mm}^2$ This reduces the lasing threshold and improves the directivity of the emission [24]. Pulsed illumination is necessary to avoid triplet state quenching of Rhodamin which suppresses lasing [25]. The laser light was detected by a multimode fiber (NA = 0.22) with a core diameter of 200 μm in in-plane direction connected to a CCD grating spectrometer (Ocean Optics HR2000) with a resolution of 0.2 nm. The fiber tip was placed approximately 100 μm from the edge of the sample. The rectangular area from the pump beam was imaged onto the polymer with a microscope objective so that no pump light was detected in the spectrometer (Fig. 4).

The cutoff condition for the propagation of TE-modes in an asymmetric, three-layer waveguide is $\Delta n > (2m+1)^2\lambda^2/(16t_g^2(n_2+n_3))$ where m is the mode order and t_g equates to the thickness of the waveguide [26]. n_2 and n_3 are the refractive indices of the waveguide and substrate, respectively. For a waveguide thickness of less than $t_g \approx 800$ nm, the device supports only the lowest-order TE-mode, but even for a thicker waveguide, the spatial loss experienced by higher modes in the grating layer may be larger, favoring lasing on the fundamental TE-mode [27]. We also measured the polarization of the laser emission with a photodiode and a polarization filter.

Figure 5 shows a typical emission spectrum of a DFB laser array with four different third-order grating pitches. The grating pitch between each device has been increased by 5 nm. Although first-order gratings are desirable for DFB lasers due to the highest performance, a third-order grating is used due to fabrication tolerances since out-of-plane coupling is much weaker than in the second-order case. The devices were fabricated side by side in a single exposure process and pumped with the same pulse energy of 3 μJ. The laser at $\Lambda = 545\,\text{nm}$ has the lowest output power since it lies at a spectral position where the gain is comparably small. The laser fabricated with $\lambda = 555\,\text{nm}$ exhibits a photoluminescent background. This is most

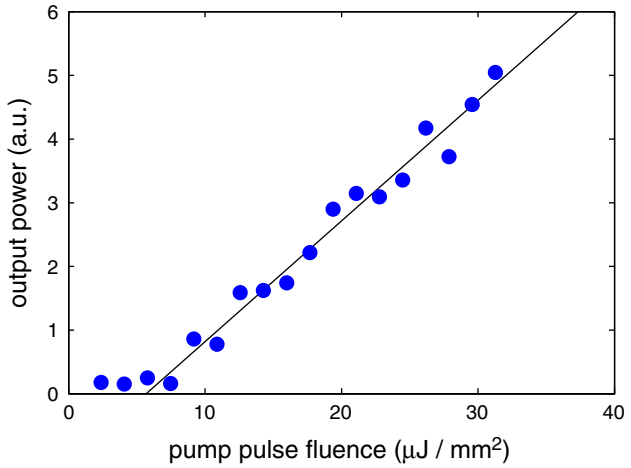

Fig. 6 Output intensity as a function of the pump pulse fluence at 10 Hz repetition rate. The lasing threshold is indicated by the linear fit

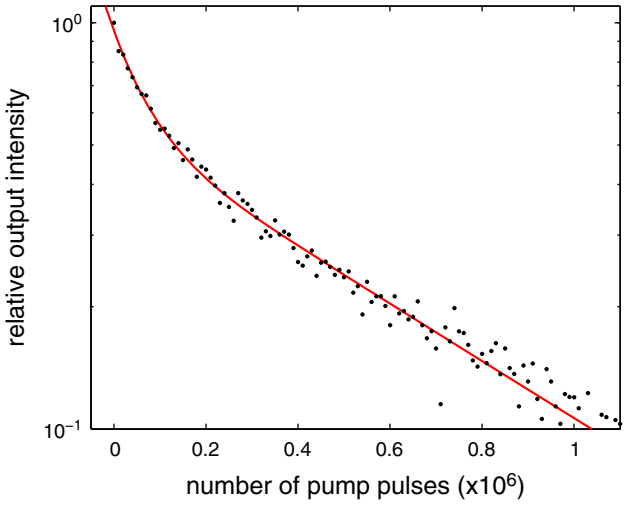

Fig. 7 Lifetime of a DFB laser pumped with 16 μJ pulse energy at 10 Hz repetition rate. The number of pump pulses where the output intensity has decreased to half of its initial value is around 1.2×10^5 pump pulses

likely due to a fabrication defects or impurities in the polymer.

The effective refractive index seen by a mode was calculated from the spectral position yielding $n_{\text{eff}} = 1.537$ for the emission peak at $\lambda = 558.5\,\text{nm}$ with a grating pitch of $\Lambda = 545\,\text{nm}$. Higher-emission wavelengths exhibit a small linear reduction in the effective refractive index with a dispersion of $-2.1 \cdot 10^{-4}/\text{nm}$. This value is a result of the material and waveguide dispersion of the laser. The measured linewidth of the emission is between $\Delta\lambda_{\text{bw}} = 300\,\text{pm}$ and $\Delta\lambda_{\text{bw}} = 400\,\text{pm}$ limited only by the spectrometer resolution and calculation by the transfer matrix method suggest a theoretical transmission bandwidth of $\Delta\lambda = 50\,\text{pm}$ in a lossless system. However, different loss mechanisms such as scattering and absorption broaden the width of the passband.

Figure 6 shows the laser output against pump power fluence, indicating the threshold behavior of the device. Below the lasing threshold, photoluminescence is present which was clearly observed on a camera by inserting a dielectric mirror to filter the pump light. The curve follows the expected linear regression, and the lasing threshold is at $6\,\mu\text{J}/\text{mm}^2$. The slope efficiency for the fabricated lasers was measured with a calibrated photodetector and was typically below 1 % without considering coupling losses and scattering. The slope efficiency therefore represents only the amount of energy collected by the fiber tip at a position where it was at its maximum value. With a more sophisticated output coupling, e.g., an undoped polymer waveguide, slope efficiency is expected to increase significantly [28]. In general a low output power is expected due to the high grating reflectivity produced by the polymer–air boundary. Additionally, the polarization ratio of the output emission that was measured above the lasing threshold exhibits a high degree of polarization of more than 20:1 in the chip plane direction, indicating lasing of the TE-mode.

Figure 7 shows a lifetime measurement of a DFB laser with a fixed pump energy of 16 μJ at 10 Hz repetition rate. The gain material in a dye-doped polymer has a limited photostability under strong pump irradiation and exhibits photobleaching, thus limiting the operational lifetime of the laser. The plot shows the measured output energy normalized to its initial value as a function of the pumping shots and fits a double exponential decay. This behavior is similar to the Rhodamin-SU-8 device reported in [13]. We observed a reduced lifetime when the device was pumped with a higher repetition rate and pump energy. For a typical device, output intensity decreases to half of its initial value after approximately 1.2×10^5 shots. We also observed increased scattering of the photoluminescent signal at the phase-slip region where a strongly confined localized mode is formed. This resonant effect increases the bleaching effect, resulting in increased photobleaching at this region and saturating the output emission.

4 Conclusion

In conclusion, we have demonstrated a DFB laser in dye-doped SU-8 fabricated by femtosecond laser writing. The fabricated devices show single-mode lasing when pumped with a pulsed Nd:YAG laser. Different lasing wavelengths were demonstrated by varying the pitch of the feedback grating. Fabrication with point-by-point femtosecond laser writing enables rapid prototyping of small light sources

suitable for integrated detection application. Furthermore, feedback gratings can be designed in three dimensions possibly allowing combination of three-dimensional high-Q resonators such as microtoroids with subwavelength surface corrugations. Organic DFB lasers can be combined in currently developed femtosecond written microfluidic/waveguide lab-on-a-chip systems with desired topography.

References

1. I.D.W. Samuel, G.A. Turnbull, Chem. Rev. **107**, 1272–1295 (2007)
2. S. Chenais, S. Forget, Polym. Int. **61**, 390–406 (2012)
3. H. Kogelnik, C.V. Shank, Appl. Phys. Lett. **18**, 152–154 (1971)
4. C. Kallinger, M. Hilmer, A. Haugeneder, M. Perner, W. Spirkl, U. Lemmer, J. Feldmann, U. Scherf, K. Müllen, A. Gombert, V. Wittwer, Adv. Mat. **10**, 920–923 (1998)
5. D. Schneider, S. Hartmann, T. Benstem, T. Dobbertin, D. Heithecker, D. Metzdorf, E. Becker, T. Riedl, H.-H. Johannes, W. Kowalsky, T. Weimann, J. Wang, P. Hinze, Appl. Phys. B **77**, 399–402 (2003)
6. T. Voss, D. Scheel, W. Schade, Appl. Phys. B **73**, 105–109 (2001)
7. X.-L. Zhu, S.-K. Lam, D. Lo, Appl. Opt. **39**, 3104–3107 (2000)
8. Y. Yang, G.A. Turnbull, I.D.W. Samuel, Appl. Phys. Lett. **92**, 163306–163306-3 (2008)
9. C. Hu, S. Kim, Appl. Phys. Lett. **29**, 582–585 (1976)
10. Y. Oki, T. Yoshiura, Y. Chisaki, M. Maeda, Appl. Opt. **41**, 5030–5035 (2002)
11. D. Nilsson, T. Nielsen, A. Kristensen, Microelectron. Eng. **73–74**, 372–376 (2004)
12. D. Nilsson, S. Balslev, M. Gregersen, A. Kristensen, Appl. Opt. **44**, 4965–4971 (2005)
13. S. Balslev, T. Rasmussen, P. Shi, A. Kristensen, J. Micromech. Microeng. **15**, 2456–2460 (2005)
14. S. Venugopal Rao, A.A. Bettiol, F. Watt, J. Phys. D. Appl. Phys. **41**, 192002 (2008)
15. G. Witzgall, R. Vrijen, E. Yablonovitch, V. Doan, B.J. Schwartz, Opt. Lett. **23**, 1745–1747 (1998)
16. T. Grossmann, S. Schleede, M. Hauser, T. Beck, M. Thiel, G. von Freymann, T. Mappes, H. Kalt, Opt. Express **19**, 11451–11456 (2011)
17. C.-F. Li, X.-Z. Dong, F. Jin, W. Jin, W.-Q. Chen, Z.-S. Zhao, X.-M. Duan, Appl. Phys. A **89**, 145–148 (2007)
18. T. Woggon, T. Kleiner, M. Punke, U. Lemmer, Opt. Express **17**, 2500–2507 (2009)
19. M.B. Christiansen, T. Buß, C.L.C. Smith, S.R. Petersen, M.M. Jørgensen, A. Kristensen, J. Micromech. Microeng. **20**, 115025 (2010)
20. H. Kogelnik, C.V. Shank, J. Appl. Phys. **43**, 2327–2335 (1972)
21. S. Riechel, U. Lemmer, J. Feldmann, T. Benstem, W. Kowalsky, U. Scherf, A. Gombert, V. Wittwer, Appl. Phys. B **71**, 897–900 (2000)
22. S. McCall, P. Platzman, IEEE J. Quantum Elect. **21**, 1899–1904 (1985)
23. T. Erdogan, J. Lightwave Technol. **15**, 1277–1294 (1997)
24. V. Dumarcher, L. Rocha, C. Denis, C. Fiorini, J.-M. Nunzi, F. Sobel, B. Sahraoui, D. Gindre, J. Opt. A-Pure Appl. Opt. **2**, 279–283 (2000)
25. S. John, G. Pang, Phys. Rev. A **54**, 3642–3652 (1996)
26. R.G. Hunsperger, *Integrated Optics: Theory and Technology* (Springer, Berlin, 2009)
27. S. Balslev, A. Mironov, D. Nilsson, A. Kristensen, Opt. Express **14**, 2170–2177 (2006)
28. M.B. Christiansen, M. Schøler, A. Kristensen, Opt. Express **15**, 3931–3939 (2007)